Provided for non-commercial research and education use.
Not for reproduction, distribution or commercial use.

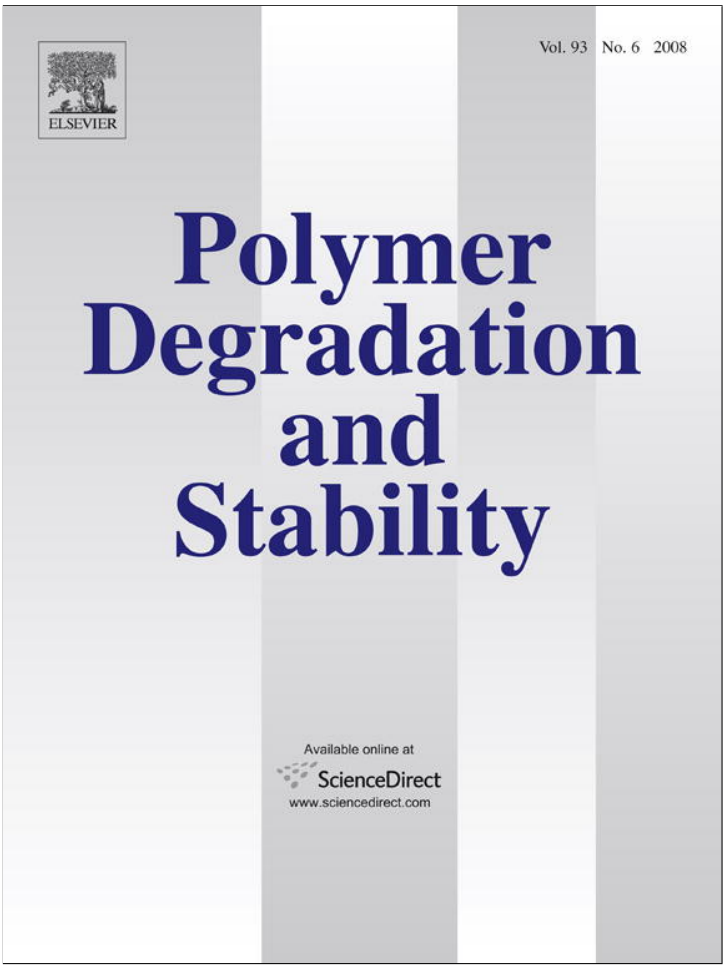

This article appeared in a journal published by Elsevier. The attached copy is furnished to the author for internal non-commercial research and education use, including for instruction at the authors institution and sharing with colleagues.

Other uses, including reproduction and distribution, or selling or licensing copies, or posting to personal, institutional or third party websites are prohibited.

In most cases authors are permitted to post their version of the article (e.g. in Word or Tex form) to their personal website or institutional repository. Authors requiring further information regarding Elsevier's archiving and manuscript policies are encouraged to visit:

http://www.elsevier.com/copyright

Author's personal copy

Polymer Degradation and Stability 93 (2008) 1081–1087

Contents lists available at ScienceDirect

Polymer Degradation and Stability

journal homepage: www.elsevier.com/locate/polydegstab

Fabrication of porous 3-D structure from poly(L-lactide)-based nano-composite foams. Effect of foam structure on enzymatic degradation

Makoto Bitou, Masami Okamoto*

Advanced Polymeric Nanostructured Materials Engineering, Graduate School of Engineering, Toyota Technological Institute, 2-12-1 Hisakata, Tempaku, Nagoya 468 8511, Japan

ARTICLE INFO

Article history:
Received 29 January 2008
Accepted 12 March 2008
Available online 18 March 2008

Keywords:
Poly(L-lactide)-based nano-composite foam
Enzymatic degradation
Porous 3-D structure
Nanocellular
Pore size distribution

ABSTRACT

To understand the effect of the foam structure on the enzymatic degradation and porous structure development, we have examined the enzymatic degradation of a poly(L-lactide) (PLLA)-based nano-composite foam having different cell density (microcellular and nanocellular), using proteinase-K as a degrading agent at 37 °C. The surface and cross-sectional morphologies of the foam recovered after enzymatic hydrolysis for different intervals were investigated by using scanning electron microscopic and mercury porosimetric analyses. The fabrication of porous three-dimensional structure for tissue engineering scaffolds and the degradation performance in nano-composite foams were discussed.

© 2008 Elsevier Ltd. All rights reserved.

1. Introduction

In our previous paper [1], we described the preparation of the porous three-dimensional (3-D) structure from a poly(L-lactide) (PLLA)-based nano-composite foam via enzymatic degradation. We specifically discussed the influence of the foam structure having high cell density (nanocellular) on the enzymatic degradation and porous structure development based on the results of the observation of scanning electron microscope (SEM). The main features of our observation were as follows [1]. In the enzymatic degradation of PLLA matrix before and after nano-composites preparation, the dispersed silicate layers had almost no effect on the acceleration of the degradation rate in the enzymatic hydrolysis. In the foam, the accelerated enzymatic degradation was caused by the large surface area inside the nanocelluar structure. The nanocelluar took up large amount of water, which led to the swelling of the foam, and thus facilitated the enzymatic degradation of matrix PLLA as compared with the bulk (pre-foamed) sample. For this reason, we have successfully prepared a porous 3-D structure as a remaining scaffold in the core part of the nano-composite foam, reflecting the spherulite of the crystallized PLLA. Thus, the degraded nano-composite foam provided the porous 3-D scaffold and the pore size was determined by controlling the degradation time using proteinase-K as an effective degrading catalyst.

However, for a better understanding of the development of the porous 3-D structure, one needs to pin down the morphological details of the enzymatic degradation of the foam structure having microcellular cell density. In this aspect, the main aim of this paper is to correlate the developed 3-D morphology after degradation *versus* foam structure with microcellular level. Then we expect the effect of the foam structure having different cell density (microcellular and nanocellular) on the enzymatic degradation and porous structure development. Such a comparison will be worthwhile not only for assessing the fabrication of porous 3-D structure for tissue engineering scaffolds but also for studying the degradation performance in nano-composite foams.

2. Experimental section

2.1. Material

The PLLA-based nano-composites used in this study were same material as in our previous studies [2]. The nano-composite was prepared through the melt extrusion method with organo-clay (montmorillonite (MMT) intercalated with octadecylammonium cation [2,3]) content of 5 wt% and henceforth will be termed as PLLACN5, using a twin screw extruder (PCM-30, Ikegai Machinery Co.) operating at 210 °C. The dried PLLACN5 pellets were converted into sheets with a thickness of 0.18 and 0.88 mm by pressing with ~1.5 MPa at 190 °C for 3 min using a hot press. The molded sheets were quickly quenched between glass plates and then annealed at 100 °C for 7 min up to 10 h to crystallize isothermally before being subjected to various characterizations and foam processing.

* Corresponding author. Fax: +81 (0) 52 809 1864.
E-mail address: okamoto@toyota-ti.ac.jp (M. Okamoto).

0141-3910/$ – see front matter © 2008 Elsevier Ltd. All rights reserved.
doi:10.1016/j.polymdegradstab.2008.03.014

Author's personal copy

2.2. Foam processing

Foam processing of PLLACN5 was conducted in an autoclave (TSC-WC-0096, Taiatsu Techno Co.) by using supercritical CO_2 [4]. Crystallized nano-composite sheet ($10 \times 25 \times 0.88$ mm^3 = width $\times$ length $\times$ thickness) was inserted into an autoclave (96 mL) and CO_2 pressure was increased up to 28 MPa for 4 h at 100 °C for nanocellular formation and at 120 °C for microcellular formation, respectively. For such a long time of CO_2 dissolution into the sample, CO_2 has already been completely saturated in the sample at fixed temperature. Subsequently, the CO_2 was quickly released from the autoclave (within 3 s). After releasing the CO_2 pressure, the formed foam was stabilized *via* cooling by liquid-CO_2 to room temperature, and then removed carefully from the autoclave and kept at ambient temperature.

The mass density of both pre-foamed ($\rho_p = 1.2620$ g/cm^3) and post-foamed (ρ_f, g/cm^3) samples were estimated by using the buoyancy method. The average cell radius (d, mm) was determined from the data of scanning electron microscopic (SEM) observation. The sample almost obeyed the Gaussian distribution. The function for determining cell density (N_c, cell/cm^3) is defined by the following Eq. (1) [4]

$$N_c = 10^4 \frac{3\left[1 - \left(\rho_f/\rho_p\right)\right]}{4\pi d^3} \tag{1}$$

On the other hand, the mean cell wall thickness (δ, μm) was estimated by the following Eq. (2) [4].

$$\delta = d\left(1/\sqrt{1 - \left(\rho_f/\rho_p\right)} - 1\right) \tag{2}$$

2.3. Enzymatic degradation

The enzymatic degradation of nano-composite foams having different cell density and crystallinity in the presence of proteinase-K was conducted according to the procedure reported by Reeve et al. [5].

For the degradation of nano-composite foams, the sheet ($10 \times 25 \times 0.88$ mm^3 = width $\times$ length $\times$ thickness) was placed in a vial filled with 5 mL of 100 mM Tris–HCl buffered solution (Nacalai Tesque) (pH 7.9) containing 0.2 mg/mL proteinase-K (Nacalai Tesque, lyophilized powder, 36.9 units/mg) and then incubated at a thermostat-controlled temperature of 37 °C in a shaker for up to 240 h. The foam was incubated for 1000 h. The hydrolysis media were changed every 24 h to maintain enzymatic activity. Specimens were withdrawn at certain intervals, and washed with distilled water to stop further enzymatic hydrolysis and then dried under vacuum at room temperature for 2 days prior to the characterization. All measurements were performed for three replicates of specimens and averaged to get the final result.

The enzymatic degradation rate of the specimens was estimated by the weight loss and normalized weight loss using the following equation:

$$\text{Weight loss}\left(\mu g/\text{mm}^2\right) = \left(\frac{W(t=0) - W(t)}{A_0}\right)\left(\frac{x_{PLLA}}{(V_{PLLA})^{2/3}}\right) \tag{3}$$

$$\text{Normalized weight loss}(\%) = 100\left(\frac{W(t=0) - W(t)}{W(t=0)}\right) \tag{4}$$

where $W(t=0)$, $W(t)$ and A_0 are the film weights before and after hydrolysis and initial surface area of the films, respectively; x_{PLLA} and V_{PLLA} correspond to weight and volume fractions of PLLA in each sample on the assumption that the ratio of PLLA/organo-MMT removed from the films is the same as that before degradation.

For the hydrolysis of nano-composite foams, we also evaluated the water absorption by the following equation:

$$\text{Water absorption}(\text{wt}\%) = 100\left(\frac{W(\text{wet}) - W(t)}{W(t)}\right) \tag{5}$$

where W (wet) is the wet weight of a specimen after degradation.

2.4. Characterization

2.4.1. Gel permeation chromatography (GPC)

The weight-average (M_w) and number-average (M_n) molecular weights of neat PLLA and PLLACN5 were determined from GPC (LC-VP, Shimadzu Co.), using polystyrene standards for calibration and tetrahydrofuran (THF) as the carrier solvent at 40 °C with a flow rate of 0.5 mL/min. For the GPC measurements first samples were dissolved in chloroform and then diluted with THF [3].

2.4.2. Differential scanning calorimetry (DSC)

The crystallized specimens were characterized by using temperature-modulated DSC (TMDSC) (TA 2920; TA Instruments) at the heating rate of 5 °C/min with a heating/cooling cycle of the modulation period of 60 s and the amplitude of ±0.769 °C, to determine heat of fusion, the DSC was calibrated with Indium before experiments [6].

For the measurement of degree of crystallinity (χ_c) prior to TMDSC analysis, the extra heat absorbed by the crystallites formed during heating had to be subtracted from the total endothermic heat flow due to the melting of the whole crystallites. This can be done according to the principles and procedures described in our previous paper [7]. In the TMDSC experiments, the endothermic heat flow $\Delta H_{different}$ of the initially existing crystallites can be easily calculated as $\Delta H_{difference} = \Delta H_{rev} - \Delta H_{nonrev}$, where ΔH_{rev} is the endothermic melting (reversing) enthalpy from the reversing heat flow profile and ΔH_{nonrev} is the exothermic ordering/crystallization (nonreversing) enthalpy from the nonreversing heat flow profile appearing in the temperature range of −30 to 200 °C. The χ_c was thus calculated as $\Delta H_{difference}/\Delta H^\circ$ with $\Delta H^\circ = 93$ J/g, which is the melting enthalpy of 100% crystalline PLLA [8].

2.4.3. Morphology

The cell structures were investigated using scanning electron microscope (SEM) (JSM-5310LV, JEOL). The samples were freeze-fractured in liquid nitrogen and sputter-coated with gold at an argon pressure of 0.1 Torr for 3 min at a current of 10 mA [3]. The surface and cross-sectional morphologies of the specimens before and after hydrolysis were also observed with a SEM. The samples were sputter-coated with gold to a thickness of ~20 nm.

The pore size and its distribution were determined by means of mercury (Hg) porosimetry (AutoPore IV-9500, Shimadzu Co.), which facilitated the pore size distribution was covered between 3 nm and 500 μm. The pore diameter (D) is defined as the following Washburn Eq. (6) [9]

$$D = \frac{-4\Gamma\cos\theta}{P} \tag{6}$$

where Γ is the surface tension of Hg, θ is the pore-Hg contact angle, and P is the applying Hg pressure up to 228 MPa. In mercury intrusion method, we estimate D value, with value of $\Gamma = 485$ mN/m and $\theta = 130°$, if we assume all pores are of identical cylindrical shape.

3. Results and discussion

3.1. Morphology of PLLACN foams

Fig. 1 shows the results of SEM images of the fracture surface (cross-section) of the PLLACN5 foamed at 100 and 120 °C (before

Author's personal copy

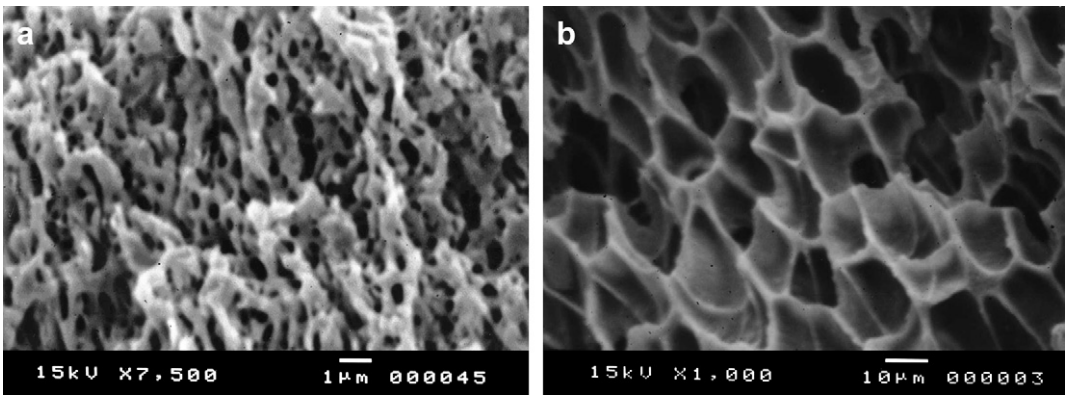

Fig. 1. SEM images of the fracture surface (cross-section) of the PLLA-based nano-composite foams: (a) nanocellular and (b) microcellular.

degradation). We noted here that both foams exhibit nicely the closed-cell structure and homogeneous cells distribution, suggesting that the dispersed silicate particles act as nucleating sites for cell formation [4]. The nano-composite foams nicely obeyed the Gaussian distribution. We have quantitatively calculated various morphological parameters of the foams: these are summarized in Table 1. In case of PLLACN5 foamed at 100 °C under high pressure of 28 MPa, the foam shows smaller cell size ($d \cong 165 \pm 7$ nm) and larger cell density ($N_c \cong 383 \times 10^{10}$ cell/cm^3) compared with that of PLLACN5 foamed at 120 °C. At low foaming temperature (100 °C), the nano-composite foam exhibits nanocellular structure, while foam prepared at 120 °C shows rather large cell structure having low cell density (microcellular).

3.2. Enzymatic degradation of foams

In enzymatic degradation, Williams [10] reported the hydrolysis of PLLA in the presence of proteinase-K, which was successfully extracted from protease in a fungus called *Tritirachium album* in 1974. This enzyme has a molecular weight of 18,500 ± 500, an isoelectric point of 8.9 and a pH optimum activity range between 7.5 and 12.0 [11]. Proteinase-K preferentially degrades PLLA over poly(D-lactide). The degradation rate significantly increases with reducing %L content from 100 to 92% in PLLA, suggesting the crystalline order dominates enzymatic degradation [5].

Fig. 2 shows the time variation of the weight (μg/mm^2) and normalized weight losses (%) of microcellular having different χ_c during the enzymatic degradation. For comparison, we also show the result of PLLACN5 (bulk sample) with $\chi_c = 44.4\%$. Obviously, the weight losses increase linearly with degradation time (t) over a period of 400 h (corresponding to 84 wt% degradation), regardless of χ_c in the matrix PLLA. A clear induction period, which is onset time until start of the weight loss in the specimen, is not observed in the microcellular degradation compared with pre-foamed PLLACN5 sample [1]. The induction time becomes longer with increasing χ_c in the bulk film (data not shown).

Fig. 3 compares the time variation of the weight loss of nanocellular structure having high χ_c value (=54.5%) [1]. To elucidate the degradation mechanism of the nano-composite foams, the linear degradation rate is estimated from the slope (d[weight loss]/dt) in the linear regime, as indicated by the solid line in Figs. 2 and 3, and is plotted as a function of the initial χ_c of the sample prior to hydrolysis in Fig. 4. For better understanding, a previous reported result on the enzymatic degradation of neat PLLA ($M_w = 3 \times 10^5$) [12] with high χ_c values and pre-foamed PLLACN5 (bulk) [1] is also

Table 1
Morphological parameters of nano-composite foams

Parameters	Nanocellular	Microcellular
ρ_f (g/cm^3)[a]	1.01	0.32
d (μm)	0.165 ± 0.072	7.55 ± 2.50
N_c ($\times 10^{-8}$ cell/cm^3)	38,300	3.81
δ (μm)	0.23	1.55

[a] ρ_p for PLLACN5 is 1.2620 g/cm^3.

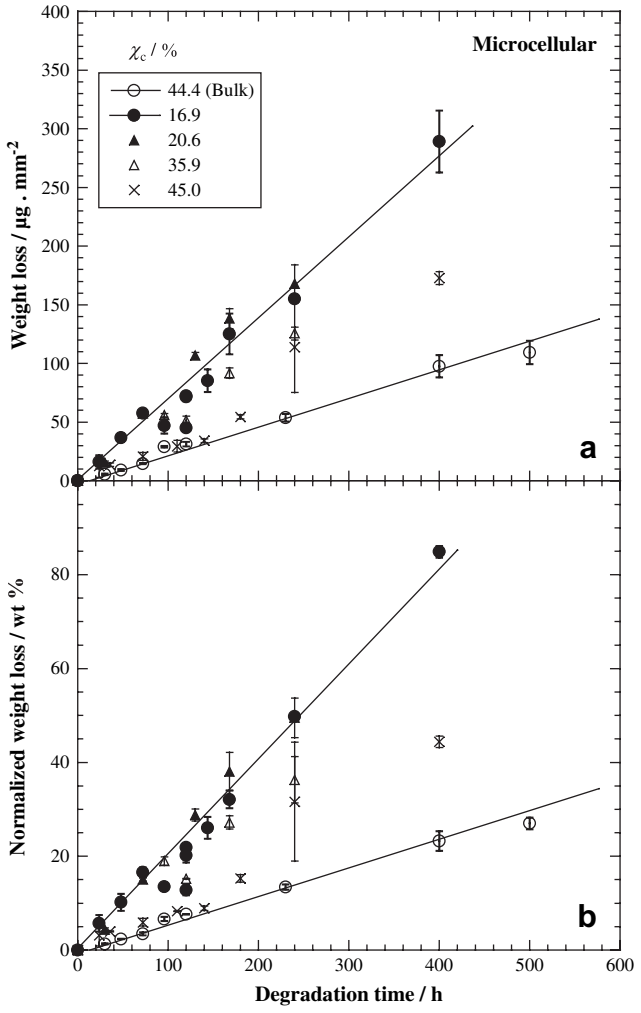

Fig. 2. (a) Weight loss and (b) normalized weight loss of microcellular having different χ_c with that of bulk data ($\chi_c = 44.4\%$) for comparison [1] during the enzymatic degradation. The solid lines are calculated by linear regression.

Author's personal copy

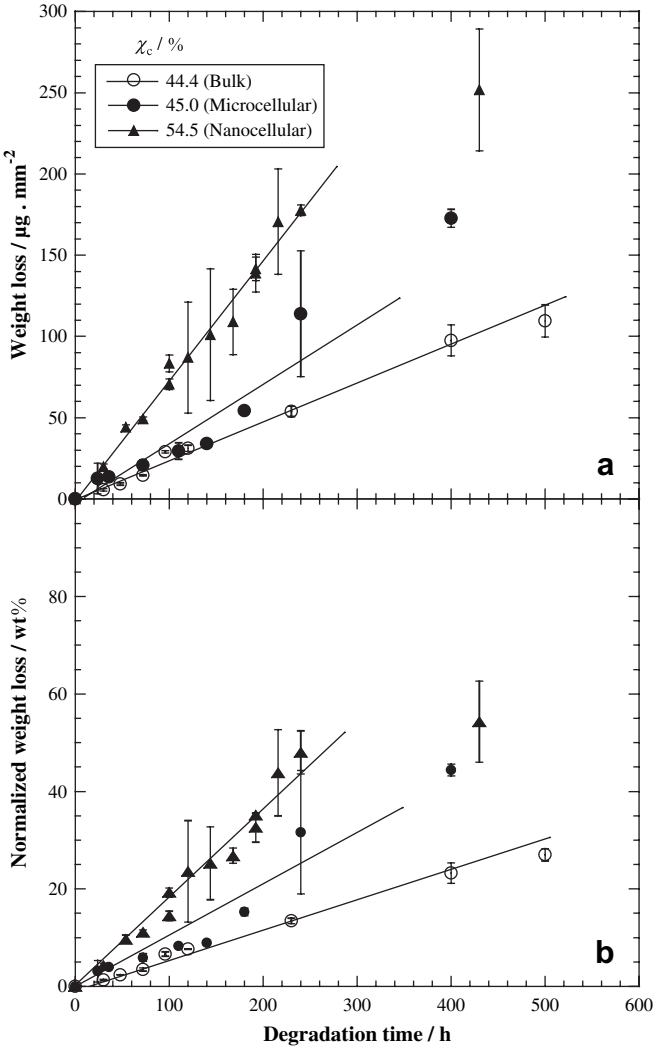

Fig. 3. (a) Weight loss and (b) normalized weight loss of nano-composite bulk, microcellular and nanocellular foams during the enzymatic degradation. The solid lines are calculated by linear regression.

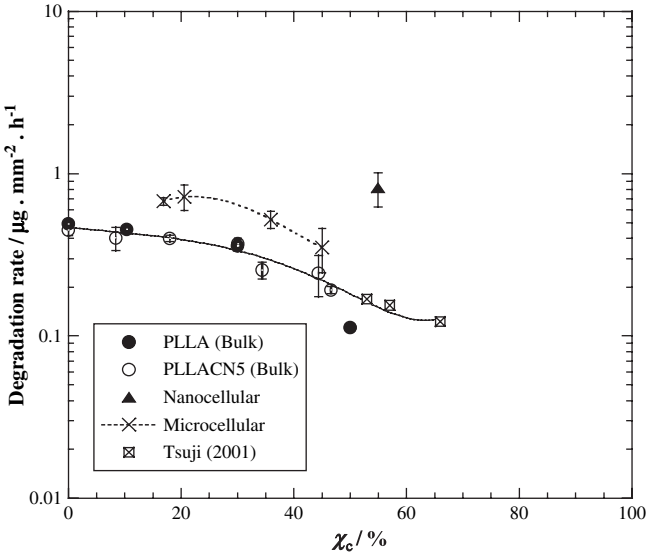

Fig. 4. Semi-logarithmic plots of linear degradation rates (μg/mm^2 h) of neat PLLA bulk, nano-composite bulk, microcellular and nanocelluar *versus* initial χ_c. Previous results on PLLA (bulk) with high χ_c values are reproduced from Tsuji et al. [15].

added in this plot. For both bulk and neat PLLA, the degradation rate slightly decreases with increasing initial χ_c in the range of 0–30%. However, the rate abruptly decreases beyond $\chi_c = 30\%$. The dispersed MMT layers have almost no effect on the acceleration of the degradation rate in the enzymatic hydrolysis of PLLACN5 as discussed previously [1].

Interestingly, the same feature has been observed in the microcellular degradation in the results of various χ_c as compared with the nano-composite bulk (and/or neat PLLA) degradation. This observation suggests that the linear degradation rate of the foams is affected by the initial value of χ_c as well as PLLACN5 (and neat PLLA) degradation reported by several researchers [5,12–14]. The enzymatic hydrolysis of matrix PLLA proceeds preferentially at disordered amorphous region on the sample surface rather than on the restricted amorphous domains, which are located between the crystalline lamellae in the spherulites [12]. The degradation rate is strongly affected by the disappearance of the free amorphous regions. This feature is also observed in the rapid increasing of the induction time [1].

3.3. Microcellular versus nanocellular

As reported by many researchers [10,12,13,15], the enzymatic degradation of matrix PLLA proceeds through surface erosion mechanism. In this process, the enzyme cannot diffuse into the film bulk. However, in the case of foams having cellular structure, the enzyme can contact with a lot of polymer chains at the cell wall surface compared with that of pre-foamed sample. As seen in Figs. 3 and 4, the linear degradation rate of the nanocellular is about two times higher than that of microcellular with same crystallinity. The accelerated enzymatic degradation in the foam is caused by the large surface area inside the nanocellular structure. From Table 1, the calculated value of the specific surface area (3.3×10^5 mm^2) is two times higher than that of microcellular (1.7×10^5 mm^2). Obviously, both the difference of the degradation rate and the difference of the surface area inside the cell structure are almost the same level for both cellular structures. This trend reflects the relative importance of the surface erosion in the enzymatic degradation of matrix PLLA, as mentioned above.

This feature is also assigned to the observation in water uptake data (Fig. 5). The nanocellular appears to uptake water much more than both microcellular and bulk. During the first 250 h, the water absorption of the foams increases continuously to attain 30% for microcellular and 50% for nanocellular. Beyond 300 h, the water uptake remains almost constant, presumably due to the saturation caused by the morphology development after enzymatic degradation. That is, the water can more easily penetrate into the foam. In contrast, PLLACN5 bulk shows very hydrophobic less than 2% of absorbed water during the degradation period. The nanocelluar takes up large amount of water compared with that of microcellular, which lead to the swelling of the foam, and thus facilitate the enzymatic degradation of matrix PLLA as compared with the bulk sample. The content of absorbed water greatly determines the enzymatic degradability [1].

3.4. Morphological change during enzymatic degradation

Fig. 6 shows the surface and the cross-section morphologies of the microcellular with $\chi_c = 16.9\%$ (Fig. 6(a)–(c)) recovered after enzymatic degradation for 400 h (corresponding to 84 wt% degradation), regardless of χ_c in the matrix of the microcellular samples. For comparison, the morphologies of the nanocellular $\chi_c = 54.5\%$ (Fig. 6(d)–(f)) and bulk sample $\chi_c = 44.4\%$ recovered after enzymatic degradation for 240 h (Fig. 6(g) and (h)) were also investigated by using SEM.

Author's personal copy

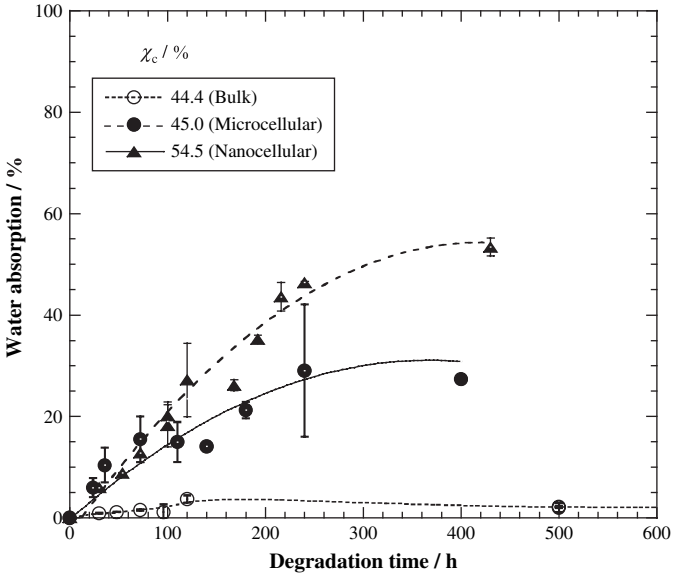

Fig. 5. Water absorption changing of nano-composite bulk, microcellular and nanocellular during the enzymatic degradation at 37 °C.

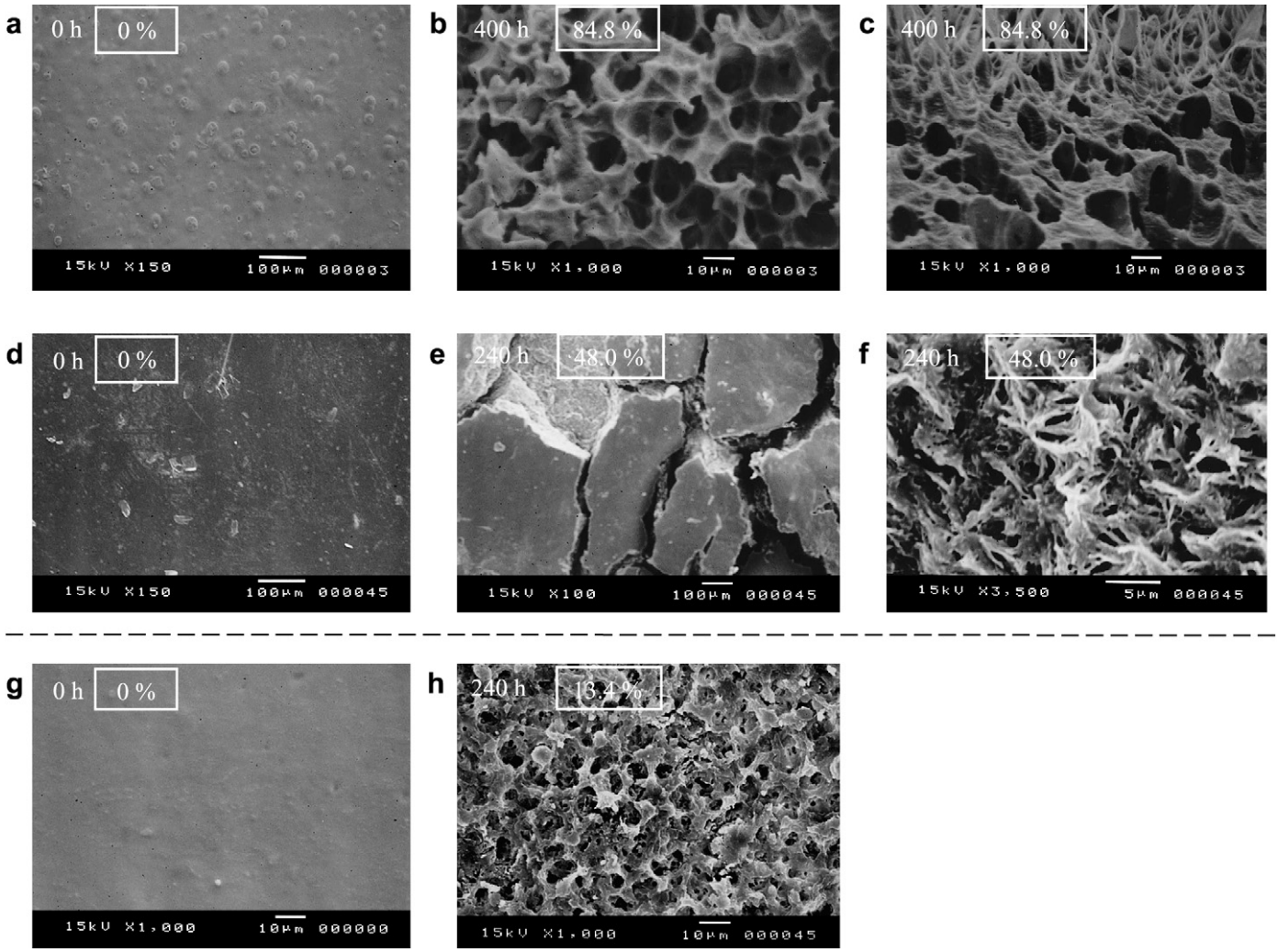

Fig. 6. Typical results of SEM images of the cross-section and the surface of microcellular (a)–(c), nanocellular (d)–(f) and nano-composite bulk (g) and (h) after enzymatic degradation for different times (240 and 400 h). The weight loss (%) of each specimen is shown by the number in the box; (c) and (f) are the cross-sectional images. The remaining are the surface images.

Author's personal copy

For the microcellular sample, a lot of pores appeared on the surface after degradation for 400 h with the diameter of ~15 μm and are polygon cell structure in shape. Interestingly, in the cross-section, the fibrillar structure with diameter of ~1–2 μm is generated on the thick cell wall ($\delta \sim 1.6$ μm) with some entanglement, suggesting that the amorphous region in the cell wall has been predominantly degraded. This structure is enhanced, as the degradation takes place.

In contrast, the surfaces of both nanocellular and bulk samples are smooth before degradation (Fig. 6(d) and (g)). For the bulk sample, a lot of pores are generated on the surface after degradation up to 120 h and the pores with diameter of ~3 μm are spherical in shape with circular interconnections (Fig. 6(h)). This kind of connected spherical-pore structure has been widely reported in the previous papers [16,17]. These holes are resulted from the degradation of the swollen (amorphous) region by the enzymatic attacks [18]. On the other hand, for the nanocellular sample, there is a great tendency to generate the skin-layer (~100 μm thickness) with cracked surface and hence more rapid fragmentation on the surface (Fig. 6(e)). No significant change, such as pore formation, on the surface during degradation up to 240 h suggests that the core part of the foam underwent significant hydrolysis during this period. This indicates that the cell structure allows the PLLA chains to become susceptible to enzymatic hydrolysis. This speculation is supported by the water uptake behavior of the nano-foam.

Fig. 6(h) presents the morphological change of the cross-section in the nanocellular after enzymatic degradation for 240 h (corresponding to 48 wt% degradation). The interesting feature is the formation of some flower-like structure [19] as a remaining scaffold in the core part, reflecting the spherulite of the crystallized PLLA. After the restricted amorphous region has been degraded, the porous 3-D scaffold left the core part in the nano-foam. This morphology of the PLLA crystals is enhanced with degradation up to 240 h. The structure size with a diameter of 10 μm observed by SEM is in good agreement with the average diameter of the spherulite developed in the sample by annealing at 100 °C before degradation [20]. The generation of the porous 3-D structure is completely different from the enzymatic degradation of bulk sample, where the morphology of the core parts remains unchanged during degradation because of the surface erosion mechanism (photo not shown). Thus, the degraded nanocellular provides the porous 3-D scaffold and the pore size is determined by controlling the degradation time using proteinase-K as an effective degrading agent, as reported in our previous paper (*cf.*, Fig. 7) [1].

3.5. Pore size and distribution

Mercury porosimetry represents a very powerful tool in the pore size distribution of small and/or large pores that are not visible in the SEM observation. In Fig. 7, we summarized the results of the pore size distribution for different degradation time taken for 0, 120 and 240 h. The *y*-axis corresponds to the pore number fraction. In the nanocellular, we see that the appearances of main peaks are observed at 40–50 nm range, which remains almost constant in the range of the degradation proceeded, whereas the appearances of small peak around 10–100 μm size is enhanced with increasing degradation time.

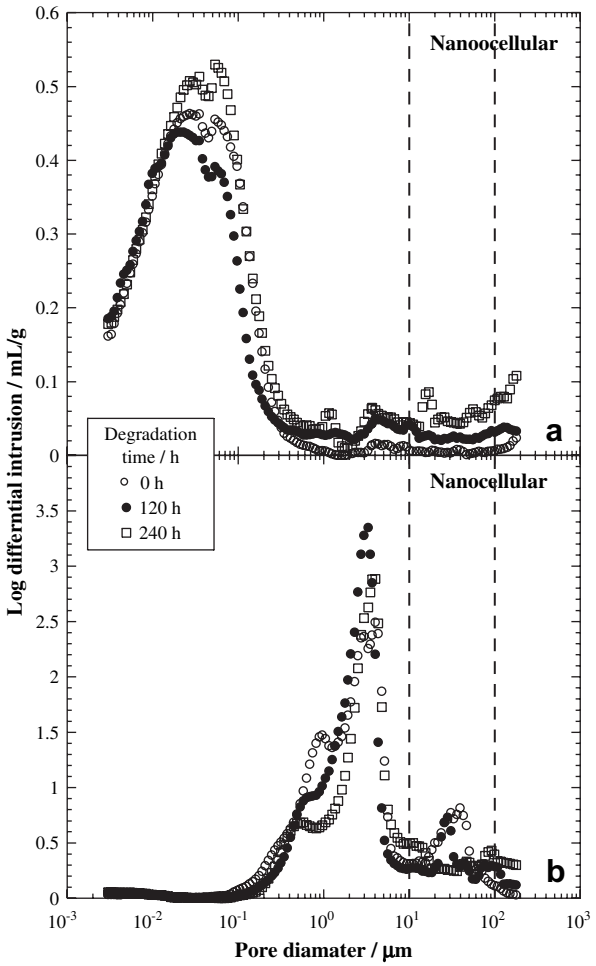

Fig. 7. Pore size distribution of (a) nanocellular and (b) microcellular after enzymatic degradation for different time intervals. The dashed lines represent the pore size range 10–100 μm.

For the microcellular, the appearances of main peaks are observed around pore size range of 3–4 μm with a small remnant shoulder around 1 μm (before degradation). As seen in nanocellular degradation, the microcellular produces pore size of 10–100 μm accompanied with decreasing of the size around 1 μm range, as the degradation takes place. This feature is not observed in the SEM images (see Fig. 6).

Thus, the combination of initial cellular structure and controlling the degradation time offers 3-D pore size controlling from nano to micrometer.

3.6. Change in the molecular weights

Table 2 summarizes the results of the thermal property, i.e., χ_c of the residual sample recovered after degradation. The residual

Table 2
Change in χ_c and M_w of residual nano-composite foams recovered after degradation

Samples	Before degradation			After degradation		
	χ_c (%)	M_w($\times 10^{-3}$ g mol^{-1})	M_w/M_n	χ_c (%)	M_w($\times 10^{-3}$ g mol^{-1})	M_w/M_n
Microcellular	16.9	113	1.71	21.9 ($t = 240$ h)	117	1.75
	45.0	113	1.71	47.1 ($t = 240$ h)	116	1.90
				46.9 ($t = 400$ h)	113	2.46
Nanocellular	54.5	121	1.70	63.1 ($t = 192$ h)	98.6	3.04

Author's personal copy

samples of both nanocellular and microcellular after enzyme exposure times of variable duration were also analyzed by GPC. After a weight loss of 49.6%, the residual microcellular shows no change in M_w. The little decreased M_w in the core part of the nanocellular is observed beyond degradation of 192 h ($M_w = 98.6 \times 10^3$ g mol^{-1}, $M_w/M_n = 3.04$) (weight loss in 30.1%). At the same time, a small increase in χ_c appears due to the preferential enzymatic degradation in the restricted amorphous region, leaving the crystalline residue. This is in agreement with the characteristics of enzymatic degradation of bulk PLLA [5,12,13], i.e., weight loss without molecular weight decrease.

4. Conclusions

In this study, we have demonstrated the enzymatic degradation of PLLA-based nano-composite foams having different cell density (microcellular and nanocellular), using proteinase-K as a degrading agent. The linear degradation rate of the microcellular was affected by the initial value of χ_c as well as nano-composite bulk degradation. The linear degradation rate of the nanocellular was about two times higher than that of microcellular with same crystallinity. The accelerated enzymatic degradation in the foam was caused by the large surface area inside the cellular structure. The nanocelluar took up large amount of water compared with that of microcellular, which led to the swelling of the foam, and thus facilitated the enzymatic degradation of matrix PLLA as compared with bulk sample. The content of absorbed water greatly determined the enzymatic degradability. For the microcellular sample, the fibrillar structure with diameter of ~1–2 μm was generated on the thick cell wall ($\delta \sim 1.6$ μm) with some entanglement as revealed by SEM observation. On the other hand, for the nanocellular sample, we have successfully prepared a porous 3-D structure as a remaining scaffold in the core part of the nanocellular, reflecting the spherulite of the crystallized PLLA.

From the pore size distribution, the appearances of 10–100 μm size were enhanced with increasing degradation time except main pore size in both nano-composite foam cases. Thus, the combination of initial cellular structure and controlling the degradation time offered 3-D pore size controlling from nano to micrometer.

Acknowledgment

This work was supported by the MEXT "Collaboration with Local Communities" Project (2005–2009).

References

[1] Bitou M, Okamoto M. Int Polym Process 2007;22:446–54.
[2] Sinha Ray S, Yamada K, Okamoto M, Ogami A, Ueda K. Chem Mater 2003;15:1456–65.
[3] Fujimoto Y, Sinha Ray S, Okamoto M, Ogami A, Ueda K. Macromol Rapid Commun 2003;24:457–61.
[4] Ema Y, Ikeya M, Okamoto M. Polymer 2006;47:5350–9.
[5] Reeve MS, McCarthy SP, Downey MJ, Gross RA. Macromolecules 1994;27:825–31.
[6] Sinha Ray S, Yamada K, Okamoto M, Ogami A, Ueda K. Polymer 2003;44:6633–46.
[7] Nam PH, Maiti P, Okamoto M, Kotaka T, Hasegawa N, Usuki A. Polymer 2001;42:9633–40.
[8] Fisher EW, Sterzel HJ, Wegner G, Kolloid ZZ. Polymer 1973;25:980–90.
[9] Smith T. Adv Colloid Interface Sci 1972;3:161–221.
[10] Williams DF. Eng Med 1981;10:5–7.
[11] Ebeling W, Hennrich N, Klockow M, Metz H, Orth HD, Lang H. Eur J Biochem 1974;47:91–7.
[12] Tsuji H, Miyauchi S. Polym Degrad Stab 2001;71:415–24.
[13] Iwata T, Doi Y. Macromolecules 1998;31:2461–7.
[14] Abe H, Doi Y, Hori Y, Hagiwara T. Polymer 1997;39:59–67.
[15] Tsuji H, Ishizaka T. Macromol Biosci 2001;1:59–65.
[16] Li S, Girard A, Garreau H, Vert M. Polym Degrad Stab 2001;71:61–7.
[17] Cai Q, Shi G, Bei J, Wang S. Biomaterials 2003;24:629–38.
[18] Fukuda N, Tsuji H, Ohnishi Y. Polym Degrad Stab 2002;78:119–27.
[19] Wang CH, Fan KR, Hsiue GH. Biomaterials 2005;26:2803–11.
[20] Nam JY, Sinha Ray S, Okamoto M. Macromolecules 2003;36:7126–31.